General Disclaimer

One or more of the Following Statements may affect this Document

- This document has been reproduced from the best copy furnished by the organizational source. It is being released in the interest of making available as much information as possible.

- This document may contain data, which exceeds the sheet parameters. It was furnished in this condition by the organizational source and is the best copy available.

- This document may contain tone-on-tone or color graphs, charts and/or pictures, which have been reproduced in black and white.

- This document is paginated as submitted by the original source.

- Portions of this document are not fully legible due to the historical nature of some of the material. However, it is the best reproduction available from the original submission.

NASA TECHNICAL MEMORANDUM NASA TM-75201

TRANSONIC FLOW PAST AN AIRFOIL WITH CONDENSATION

B. Schmidt

(NASA-TM-75201) TRANSONIC FLOW PAST AN AIRFOIL WITH CONDENSATION (National Aeronautics and Space Administration) 21 p HC A02/MF A01 CSCL 01A

N78-19053

Unclas
G3/02 08645

Translation of "Schallnahe Profilumströmung mit Kondensation", Acta Mechanica, Vol. 2, 1966, pp. 194-208.

NATIONAL AERONAUTICS AND SPACE ADMINISTRATION
WASHINGTON, D.C. 20546 MARCH 1978

STANDARD TITLE PAGE

1. Report No.	2. Government Accession No.	3. Recipient's Catalog No.
NASA TM-75201		

4. Title and Subtitle	5. Report Date
TRANSONIC FLOW PAST AN AIRFOIL WITH CONDENSATION	MARCH 1978
	6. Performing Organization Code

7. Author(s)	8. Performing Organization Report No.
B. Schmidt	
	10. Work Unit No.

9. Performing Organization Name and Address	11. Contract or Grant No.
SCITRAN Box 5456 Santa Barbara, CA 93108	NASw-2791
	13. Type of Report and Period Covered
	Translation
12. Sponsoring Agency Name and Address	14. Sponsoring Agency Code
National Aeronautics and Space Administration Washington, D.C. 20546	

15. Supplementary Notes

Translation of: "Schallnahe Profilumströmung mit Kondensation", Acta Mechanica, Vol. 2, 1966, pp. 194-208. (A66-39697)

16. Abstract

In connextion with investigations conducted to determine, the influence of water vapor on experiments in wind tunnels, the question arose as to what changes due to vapor condensation might be expected in airfoil measurements.

Density measurements on circular-arc airfoils aided by an interferometer in choked tunnels with parallel walls show that increasing humidity produces increasing changes in the flow field. The flow becomes nonstationary at high humidity.

At the airfoil, however, the influence of the condensation is only felt, inasmuch [as] the shock bounding the local supersonic region moves upstream with increasing humidity while its intensity decreases. The density distribution upstream of the shock remains unchanged. Even if the flow becomes nonstationary in the vicinity of the airfoil, no changes occur at the airfoil -- the base of the shock included. This is a somewhat surprising and unexpected result.

17. Key Words (Selected by Author(s))	18. Distribution Statement
	Unclassified - Unlimited

19. Security Classif. (of this report)	20. Security Classif. (of this page)	21. No. of Pages	22.
Unclassified	Unclassified		

TRANSONIC FLOW PAST AN AIRFOIL WITH CONDENSATION

B. Schmidt

SUMMARY /194*

In connection with investigations conducted to determine the influence of water vapor on experiments in wind tunnels, the question arose as to what changes due to vapor condensation might be expected in airfoil measurements.

Density measurements on circular-arc airfoils aided by an interferometer in choked tunnels with parallel walls show that increasing humidity produces increasing changes in the flow field. The flow becomes nonstationary at high humidity.

However, the influence of the condensation is only felt at the airfoil, inasmuch as the shock bounding the local supersonic region moves upstream with increasing humidity while its intensity decreases. The density distribution upstream of the shock remains unchanged. Even if the flow becomes nonstationary in the vicinity of the airfoil, no changes occur at the airfoil - the base of the shock included. This is a somewhat surprising and unexpected result.

INDEX OF NOTATIONS USED

c	- speed of sound
$c_p = \frac{p - p_\infty}{\frac{1}{2}\varrho_\infty u^2_\infty} \approx -2\varphi_x$	- pressure coefficient
$c_p^* = \frac{(\varkappa+1)^{1/3}}{\tau^{4/3}} c_p$	- standardized pressure coefficient
d	- maximum airfoil thickness /195
H	- tunnel height (from airfoil centerline to tunnel wall)

*Numbers in margin indicate pagination in foreign text.

L	- length of airfoil
M	- Mach number
p	- pressure
u	- velocity in the x-direction
x	- airfoil abscissa (station)
x [sic]	- absolute humidity of the air (in kg of water per kg of dry air)
ϕ	- perturbation potential
$\phi_x = \partial\phi/\partial x = u/c^* - 1 \approx M^* - 1$	- perturbation velocity in the x-direction
χ	- ratio of specific heats
ρ	- density
$\tau = d/L$	- normalized airfoil thickness
$\xi = x/L$	normalized airfoil coordinate (station)

Indices

0 - rest conditions

∞ - free-stream (unperturbed) conditions

* - referred to conditions at M = 1

I. INTRODUCTION

Based on the research done at this institute on the influence of air humidity on the flow field in a Laval nozzle [Refs. 1, 2], the question arose whether similar influences of humidity occur in the flow about wings. Observations of condensation phenomena for wings have been made [Ref. 3] but do not shed any light on the questions raised here.

Simple preliminary investigations using Schlieren photography clearly show /196
(Figures 1, 2) that, for a flow about a circular-arc airfoil represented by a half-model, the effect of air humidity is to change the shock configuration at the wing. Subsequent studies yielded quantitative results on the details and are described below. In particular, high air humidity can lead to nonstationary flow phenomena

in the vicinity of the wing. This, in turn, might lead to nonstationary forces acting on the wing, which is important in practical applications.

Construction of the Test Facility

The measurements and photographs were made in a wind tunnel at the Institute for Flow Studies and Flow Mechanisms of the Technical University at Karlsruhe, designed for intermittent operation (diagrams in Figures 3, 4).* The pressure drop required for the operating of the tunnel was obtained by pumping down a bank of tanks with a total volume of 34 m^3. Air of a given humidity was stored in polyethylene balloons with a volume of about 18 m^3 located upstream from the intake tube. The test section proper had parallel walls and measured between 35 x 100 mm and 35 x 150 mm and was within the field of view of the optics. The circular-arc airfoil in the test section was either a half-model attached to the upper tunnel wall or a symmetrical wing at zero angle of attack located in the center and glued to the observation ports. Upstream from the airfoil, the boundary layer could be sucked off through seven slits 1 x 40 mm each, which terminated 10 mm in front of the wing. The amount of suction could be held constant during the observation period and was chosen so that all but about 0.25 mm of the boundary layer was removed. A variable nozzle installed about 0.7 meter downstream from the test section was used to control the Mach number of the incident flow. The Mach number for the wing was varied from subcritical values up to the choking of the tunnel. For $\tau = 0.1$, $H/L = 2$, and $H = 150$ mm, the corresponding range was from $M_{\infty critical} \approx 0.78$ and $M_{\infty choke\ flow} \approx 0.83$.

/197

A manually operated ball valve with a nominal size of 200 mm served as the shut-off device for the tanks and could be opened or closed in 0.2 second. The following parameters were measured: Static pressure using a pitot tube and static tube;

---

*I am grateful to Mr. H. Lehmann for his help in conducting the research and evaluating the photographs.

static pressure at the side walls along the axis of the tunnel and at 15 to 20 mm upstream from the edge of the field of view; static pressure at the half-model attached to the wall for values of ξ = 0.25, 0.5, and 0.75; density distribution in the field of view using a Mach-Zehnder interferometer; and air humidity of the supply air in the balloons by using an aspiration psychrometer.

All pressures were measured by mercury U-tube manometers, whose connecting tubes to the test section were opened for only about 10 seconds during the stationary flow phase. The Schlieren and interferometer photographs were all made using spark photography with an exposure time of about 10^{-6} seconds. At the times when nonstationary processes were expected, slow-motion films with a frame frequency of 10^4 frames per second were made. /198

II. CIRCULAR-ARC AIRFOILS IN DRY AIR

In operating the tunnel with dry air, we can assume isentropic flow up to the conditions where compression shocks appear. The density distribution in the field of observation, determined with the interferometer, can be used to determine the corresponding Mach number distribution.

If the values of the perturbation parameter $\phi_x \approx M^* - 1$ as evaluated at the airfoil are plotted as a function of wing chord ξ, we find that the values obtained in this tunnel are above the theoretical curve given by Spreiter and Alksne [Ref. 4] for an infinitely expanded flow field. The correspondence of these measured values with the measurement results from other authors [Refs. 5, 6] is not fully satisfactory.

Simultaneously with the optical density measurements, the static pressure was measured at the airfoil for ξ = 0.25, 0.5, and 0.75. If pressure and density measurements are compared with each other at corresponding points, then we find systematic deviations between the measurements, if we assume that the local supersonic /199

region is enclosed by a compression shock sufficiently far down stream. The primary reason for these deviations is the boundary layer that exists at the observation windows. The static pressure in the boundary layer at the tunnel windows remains constant in a direction normal to the flow and along the direction of the light, while the temperature rises to approximately 80 percent of the temperature of the air at rest. Based on the equation of state, the density in the boundary layer must therefore decrease. This means that there is a small additional deflection of fringes in the interferometer image in the direction of increasing fringe deflection. The interference fringe image, when evaluated, leads to higher Mach numbers.

Thickness and profile of the boundary layer at the window panes are unknown. Correction values can be estimated by using the assumption that the boundary layer over the tunnel windows is the same in thickness and profile as that which exists upstream of the airfoil without boundary-layer suction.

Applying this correction produces good agreement between pressure and density measurements at the pressure-measurement points on the wing. Following correction, /200 the differences are about 2 percent. In the ϕ_x, ξ diagram, applying this correction results in displacing the curves by $\Delta\xi \approx 0.03$ to the right. Applying the correction improves the agreement of the measured values with the results from other publications [Refs. 4-6] (Figure 5).

In order to apply the measured values obtained for the choked tunnel to conditions of airfoil flow in free space, it is necessary to apply a tunnel correction, whose computation is difficult in the transonic region and has so far been possible only for special cases [Ref. 7]. Consideration of these special cases indicates that values measured for a choked tunnel under conditions when the tunnel is wide enough ($H/L \gtrsim 2$, $\tau \lesssim 0.1$) are in better agreement with values for the flow in free space than those obtained with the aid of perforated or slotted transonic tunnels [Ref. 8].

The problem of tunnel corrections will not be considered further. The measured values obtained here for dry air will only be used for comparison with those for humid air and are compared to known measurement results only for control purposes.

Tests using a circular-arc airfoil glued in mid-tunnel were not carried beyond /201
the preliminary stages, because the small size of the models necessitated by the small tunnel height allowed only the development of a laminar boundary layer over /202
the model. The shock configuration for an airfoil with laminar boundary layer displays quite a different picture from an airfoil with turbulent boundary layer (Figures 7, 8) [Ref. 9]. Thus, an additional and undesirable parameter would have to be considered in the studies. It is for this reason that the studies were only made /204
with a half-model that was located at the tunnel wall and that always had a developed turbulent boundary layer.

One other phenomenon should be pointed out, which was observed for airfoils located 'n the middle of the tunnel. When the incident flow Mach number approaches the choke Mach number, nonstationary processes readily appear in the test section. They show up as an alternating movement of the shock waves enclosing the local supersonic region (Figure 9). Presumably, the tunnel alternately chokes, a phenomenon which is initially expected in the vicinity of the test section choking and /205
which is easily triggered through minute asymmetries in the flow field (for example, asymmetrical separation at the airfoil or small angles of attack of the airfoil).

III. CIRCULAR-ARC AIRFOIL IN HUMID AIR

In contrast to the tests with dry air, the adjustable nozzle located downstream from the test section was fully opened and left that way for all tests using humid air. The humidity of the air was varied in the range from $0 \leq x < 0.016$ kg water/kg air using mixing inside the balloons located upstream from the intake opening.

The interferograms for these tests clearly show the changes in density distribution in the flow field for increasing values of humidity (Figures 10a-10h). The shock wave bounding the local supersonic region moves slowly upstream with increasing humidity and becomes weaker, so that, after a certain humidity is reached, the shock can no longer reach the opposite wall of the tunnel. Up to this point, the changes are quite similar to those observed for dry air for decreasing incident flow Mach number. For the tests made with humid air, the incident flow Mach number decreases only slightly from $M_\infty \approx 0.83$ for $x = 0$ kg water/kg air down to $M_\infty \approx 0.81$ with $x = 0.01$. When humidity increases to reach a value of $x \approx 0.007$, a second shock is formed, which does not reach the airfoil at the point upstream from the shock bounding the supersonic region. The new shock is at times somewhat longer than the one that follows it and could be the result of strong condensation phenomena within the local supersonic region. Ackeret, Feldmann, and Rott [Ref. 9] observed similar double-shock configurations for a curved wall and suspected water vapor condensation as the cause.

When the humidity of the air finally exceeds the value of $x \approx 0.012$, the shock system becomes nonstationary (Figure 11). Shock II, which bounds the local supersonic region, begins to move upstream starting with its whip-like end away from the airfoil, while Shock I, which lies further upstream, becomes nonstationary and grows weaker as it moves upstream and finally disappears completely. After Shock II has moved some distance upstream, it also becomes weaker with the flow accelerating behind it, and a new shock, enclosing the local supersonic region, is formed; this is Shock II_1. The original Shock II now takes on the role of the former Shock I, and thus becomes Shock I_1. This process continues as we described above and is periodic.

If one follows the line of constant density $\rho/\rho_0 = 0.6339$, which, for upstream isentropic flow, has a Mach number of 1 and thus represents the sonic line for these assumptions, we observe the following (Figures 12, 13):

For the range $0 \leq x < 0.009$, the sonic line thus defined reaches the opposite wall at a point slightly downstream. Only downstream from the sonic line can we notice changes in the density distribution due to increasing humidity.

For $x \gtrsim 0.009$, the picture changes in that the line $\rho/\rho_0 = 0.6339$, which starts /206
from the airfoil at $\xi \gtrsim 0.25$, no longer reaches the opposite wall. For air humidities above $x \gtrsim 0.009$, it is bent back toward the airfoil in the direction of the airfoil wall, after which it again bends and reaches the wall opposite the airfoil. This occurs if there is no collision with a shock. The line $\rho/\rho_0 = 0.6339$ thus assumes an S-shaped form, and we can state with confidence that this line no longer corresponds to $M = 1$ following the first deflection. The bending of the line $\rho/\rho_0 = 0.6339$ is a result of heat addition through condensation downstream from the first part of this line. The flow in the condensation area is no longer isentropic, thus making it possible to determine the sonic line without additional data on heat addition.

Should the density distribution (ρ/ρ_0) along the airfoil be plotted as a function of ξ, the following picture evolves: For increasing humidities x, the shock bounding the local supersonic region moves upstream (Figure 6). Ahead of the shock, all density curves lie within the statistical uncertainties given by the bounds of measurement accuracy. Within this range, the effect of condensation is not noticeable. Even the double-shock configuration, as shown in Figure 10f, makes itself noticed by the strong flattening of the density decrease immediately upstream from the shock (Figure 6, curve $x = 0.0093$). The addition of heat in the field above the airfoil has only a minor effect on the density distribution across the airfoil upstream from the shock.

The family of curves evaluated for humid air strongly resembles that obtained for dry air (cf. Figures 5, 6). For the dry air tests, the incident flow Mach number was varied by using the second constriction in the range from $M_{critical} \approx 0.78$ to $M_{choke} \approx 0.83$, while for the test with humid air, as we have mentioned, the incident flow Mach number was changed only due to increasing humidity in the range $M_\infty \approx 0.83$ to $M_\infty \approx 0.81$. Thus, the moving ahead of the shock as a function of increasing humidity cannot be explained by the reduction of the incident flow Mach number. The decrease in Mach number upstream from the shock as a consequence of heat addition through condensation is probably its chief cause. The effect of increasing the amount of heat added that accompanies increasing air humidity is clearly shown in the shrinking of the local supersonic region. The fact that the incident flow Mach number M_∞ is barely changed with increasing amounts of heat added indicates that the predominant portion of the heat addition occurs downstream from the sonic line. Heat addition in the wind tunnel upstream from the sonic line results in a decrease of the flow mass. In this case, the incident flow Mach number would thus have to decrease. The slight decrease observed in the incident flow Mach number for increasing air humidity could be caused by weak condensation phenomena upstream from the sonic line. The density measurements carried out make it impossible to determine the Mach number under anisentropic flow conditions; therefore, we can only guess what happened here.

/207

Above $x \approx 0.012$, the flow becomes nonstationary, especially in the flow field above the airfoil (Figure 11). The pressure oscillations caused by the moving shock waves are, surprisingly, only barely noticeable at the airfoil itself. The airfoil is reached only by the shock bounding the local supersonic region. This shock exhibits such small motions at its point of attachment that we can say that

the motions are within the range of statistical uncertainties of the measurement itself. The density distribution over the airfoil upstream from the shock is also /208 almost invariant up to a short distance upstream from the shock itself. The non-stationary phenomena thus take place only in the flow field and have very little effect on the flow conditions at the airfoil itself. This result could not have been suspected from the Schlieren photographs, which clearly show a shock configuration at variance with photographs made when dry air was used as the medium in the wind tunnel (Figures 1, 2).

IV. CONCLUDING REMARKS

I would like to thank Professor Zierep and Dr. Euteneuer for their lively interest and many suggestions during the tests.

I also thank the German Research Society for making the interferometer available to me along with the optical system and spark photography equipment used with it.

BIBLIOGRAPHY

1. Steffen, H.-H., "Interferometric Density Measurements in Airflows Through Laval Nozzles with Energy Addition Using Water Vapor Condensation," Thesis, Technical University at Karlsruhe, 1961.
2. Schmidt, B., "Observations of Perturbations Caused by Water Vapor Condensation in a Supersonic Windtunnel Nozzle," Dissertation, Technical University at Karlsruhe, 1962, 1962 Yearbook of WGLR, pp. 160-167.
3. Head, R. M., "Investigations of Spontaneous Condensation Phenomena," Dissertation, Calif. Inst. of Techn., Pasadena, Calif., 1949.
4. Spreiter, J. R., and Alksne, A. Y., NACA Rep. 1359, 1958 (supersedes NACA T. N. 3970).
5. Knechtel, E. D., NASA TN D-15 (1959).
6. Michel, R., Marchand, F., and LeGallo, J., ONERA Publ. No. 65, 1953, and ONERA Publ. No. 72, 1954.
7. Marschner, B. W., Journ. Aero Sci., 23, No. 4, 1956.
8. Spreiter, J. R., Smith, D. W., and Hyett, B. J., NASA T. R. R-73, 1960.
9. Ackeret, J., Feldmann, F., and Rott, N., "Research on Compression Shocks and Boundary Layers in Rapidly Moving Gases," Communications of the Institute for Aerodynamics of the ETH, Zurich, Issue No. 10, 1946.

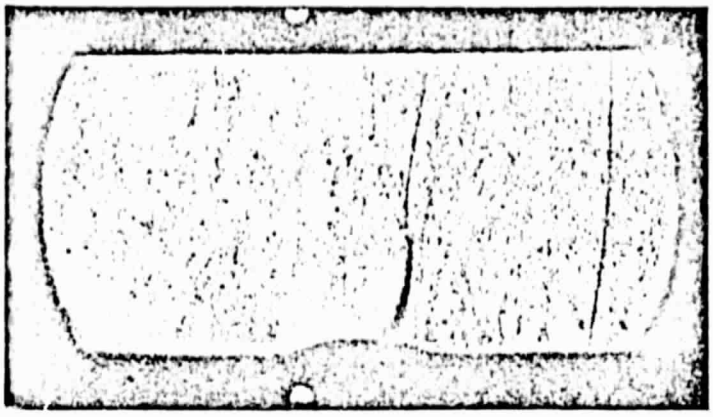

Figure 1. Dry Air. Half-model attached to wall with τ = 21%, L = 50 mm, and H = 100 mm

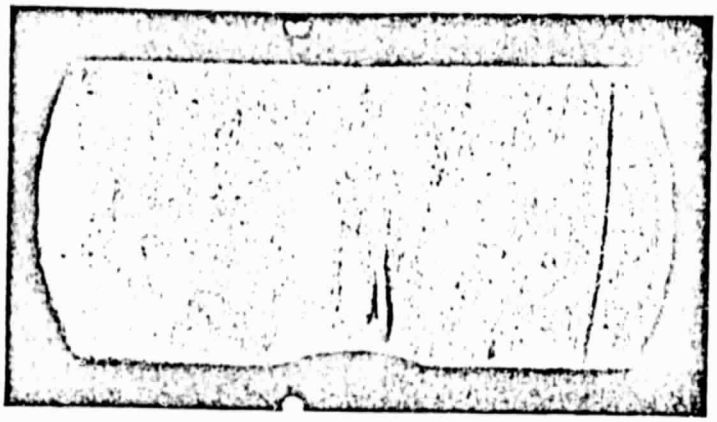

Figure 2. **x** = 0 0112. Half-model attached to wall with τ = 21%, L = 50 mm, and H = 100 mm

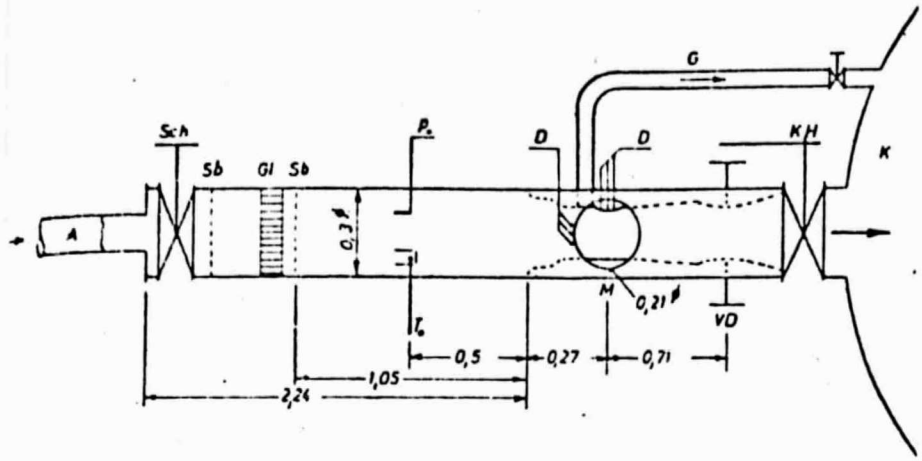

Figure 3. Schematic Diagram of Wind Tunnel. Dimensions are in meters.

Key:

A. Intake tube of 0.175 m diameter from the balloons (18 m^3)
D. Static-pressure measuring-stations
G. Boundary-layer suction
Gl. Straightener
K. Tank (34 m^3)
KH. Tank valve of 0.2 m diameter
M. Test section
P_o. Pitot tube for total pressure measurement
Sb. Screen
Sch. Gate valve of 0.3 m diameter
T_o. Temperature-sensing element for measuring temperature at rest conditions
VD. Adjustable nozzle

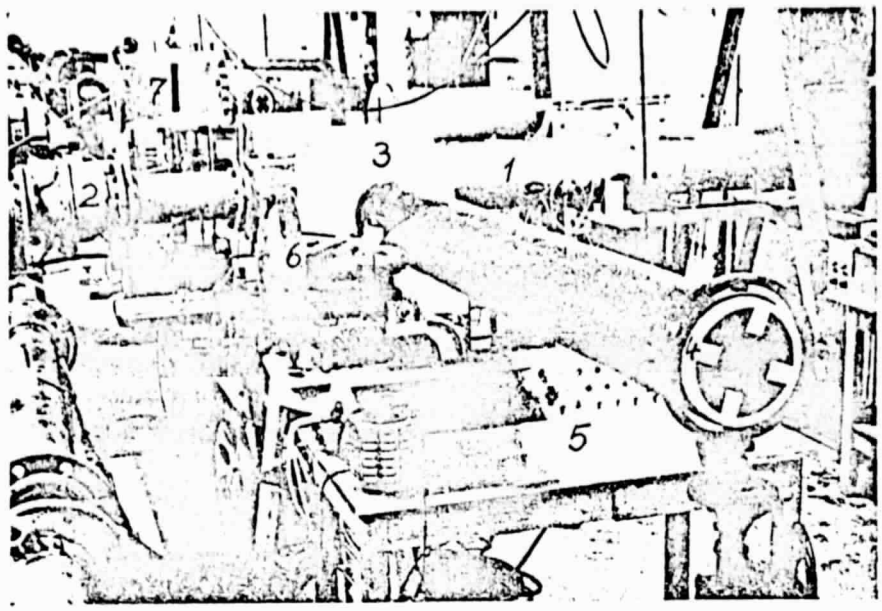

Figure 4. Test Setup as Seen From the Camera Side

Key:

1. Windtunnel intake tube
2. The NW 200 ball valve
3. Interferometer and enclosed test section
4. Concave mirror
5. Interferometer control console
6. Drum Camera
7. Completed adjustable nozzle

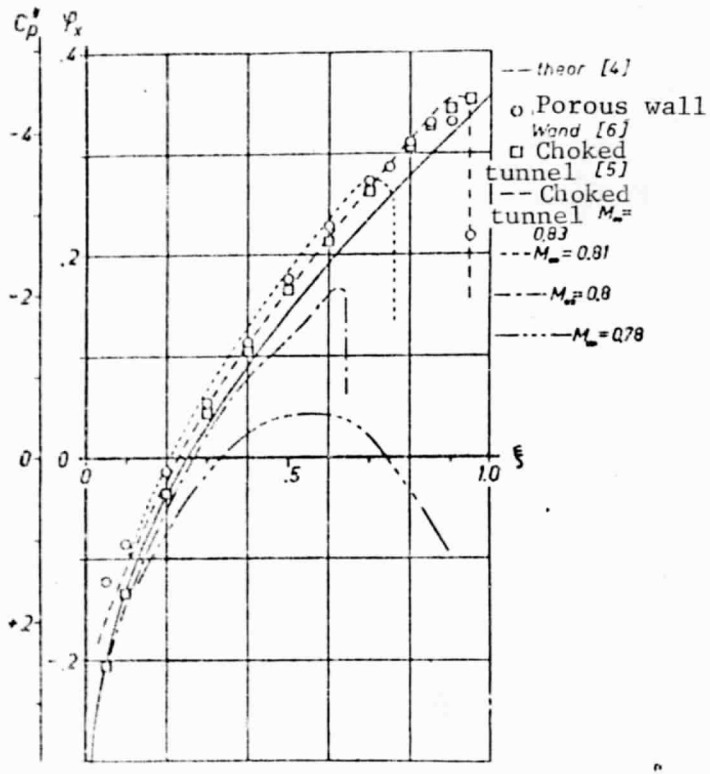

Figure 5: Test Results for Dry Air and Comparison with Known Studies

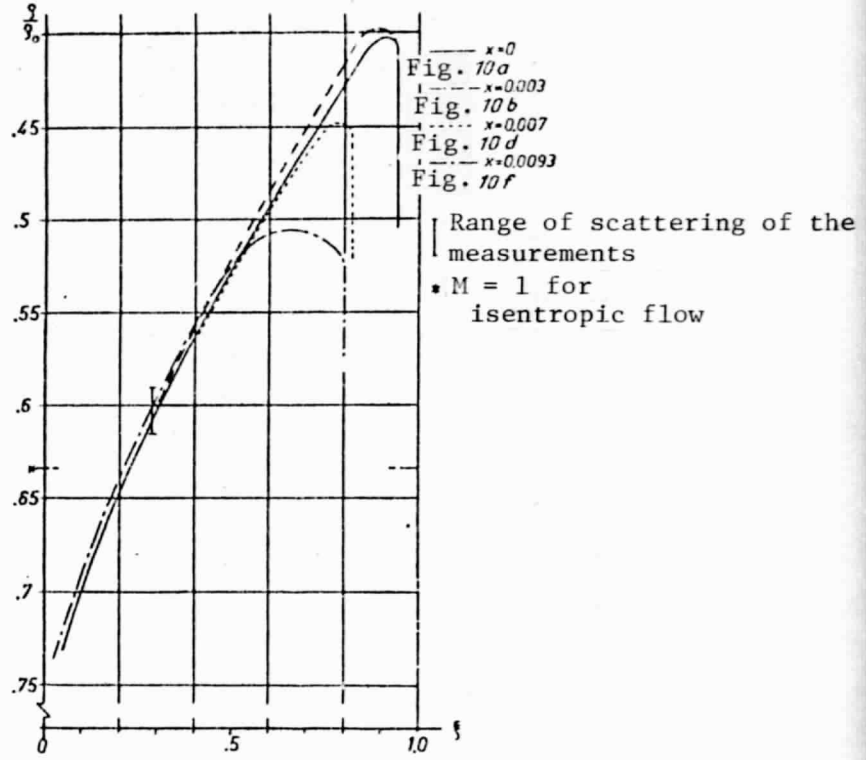

Figure 6: Test Results for Humid Air

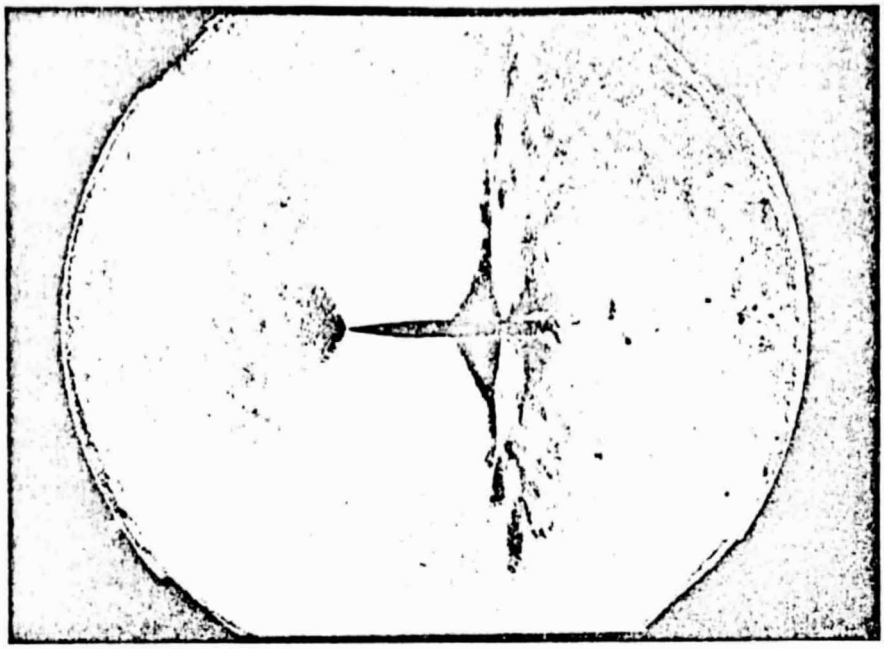

Figure 7. [Flow with] τ = 10%, L = 50 mm, 2H = 173, Dry [Air], Laminar Boundary Layer at the Airfoil, and Choked Tunnel

Figure 8. [Flow with] τ = 10%, L = 75 mm, H = 150 mm, Dry [Air], Laminar Boundary Layer at the Airfoil, and Choked Tunnel

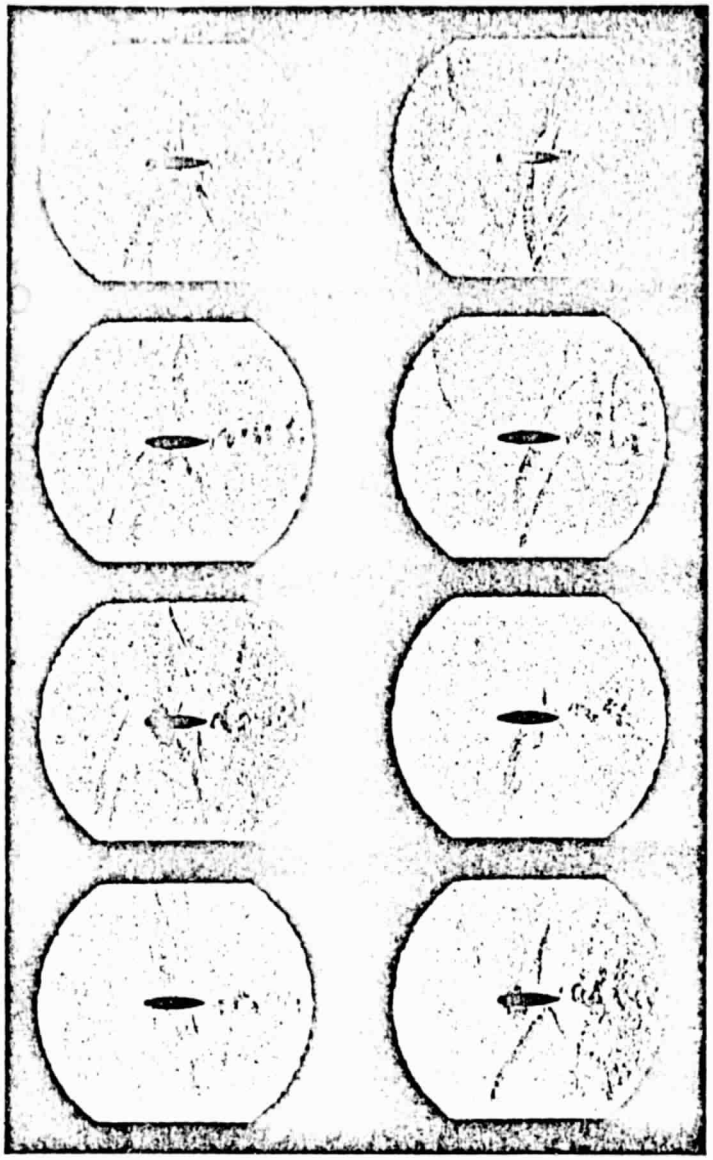

Figure 9. Circular-arc Airfoil, Dry Air, τ = 20%, $M \approx M_{choke}$, L = 50 mm, 2H = 190 mm

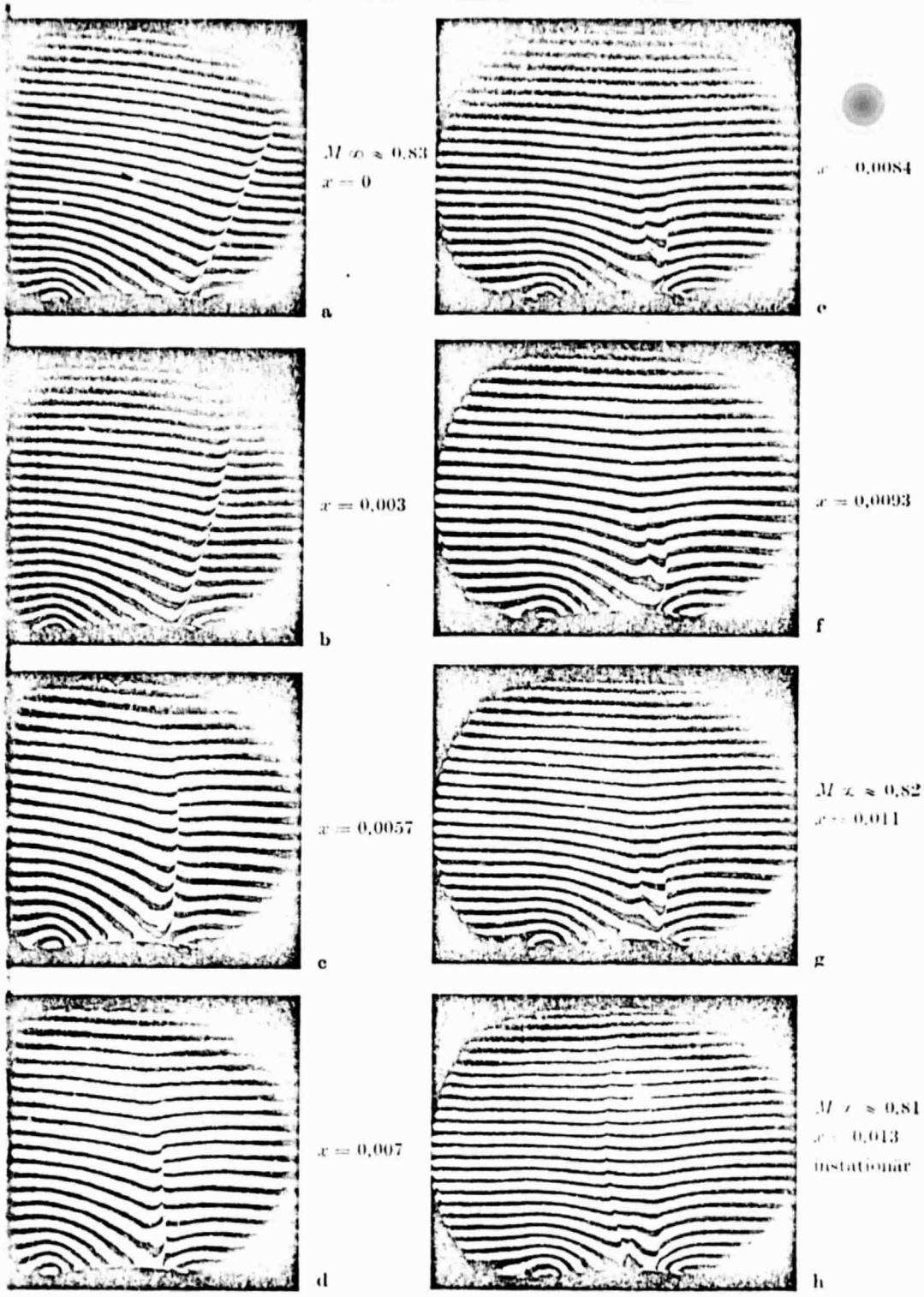

Figure 10, a-h. Circular-arc Airfoil, τ = 10%, Humid Air, H = 148 MM, L = 75 mm, Boundary Layer Sucked off Upstream from Airfoil

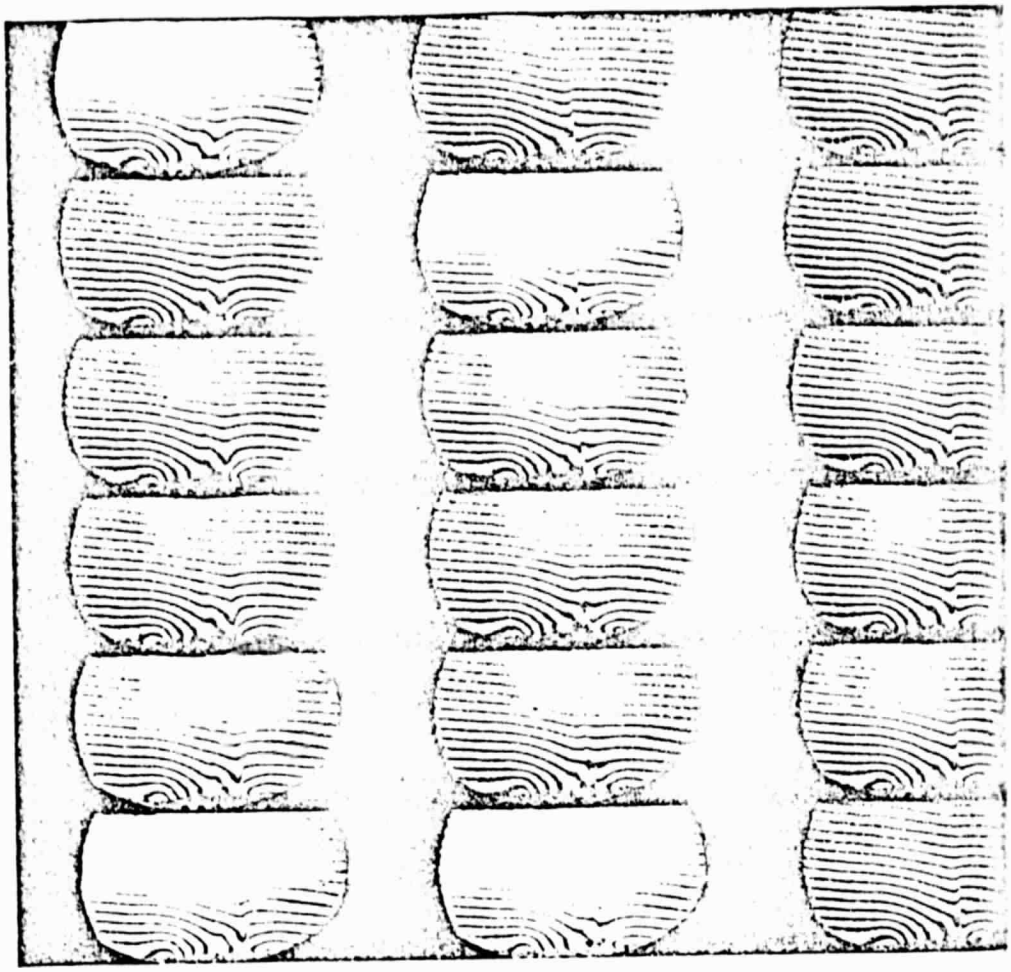

Figure 11. [Flow with] τ = 10%, H = 148 mm, L = 75 mm, x = 0.017 kg_{water}/kg_{air}, $M_\infty \gtrsim 0.81$, Boundary Layer Sucked off Upstream of Airfoil. [Film speed] 10,000 frames per second

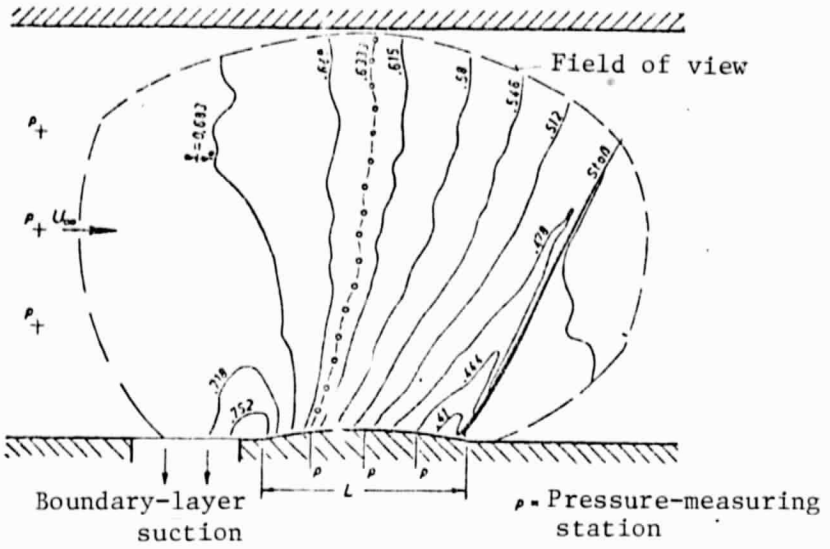

Figure 12. Density distribution for x = 0, τ = 10%, H = 148 mm, L = 75 mm, and $M_\infty \gtrsim 0.83$.

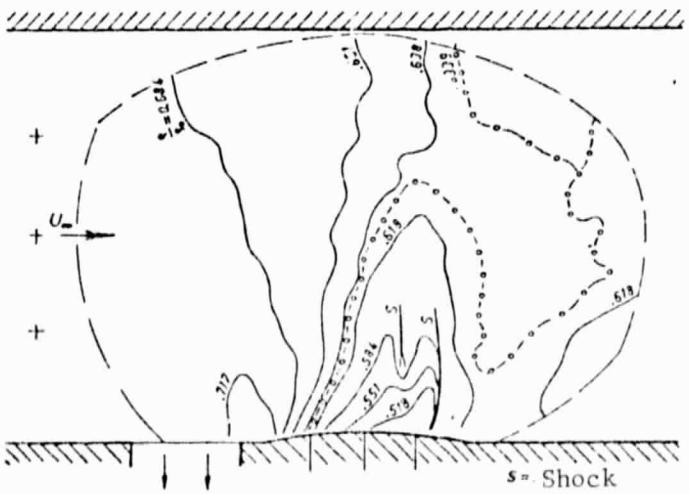

Figure 13. Density distribution for $X \gtrsim 0.010$, τ = 10%, H = 148 mm, L = 75 mm, and $M_\infty \gtrsim 0.81$.